Visnyk NTUU KPI Seriia – Radiotekhnika Radioaparatobuduvannia, 2024, Iss. 97, pp. 20–29

UDC 621.3:519.2

One-Bit Spectrum Sensing Peculiarities

Buhaiov M. V.

S. P. Korolov Military institute, Zhytomyr, Ukraine

E-mail: *karunen@ukr.net*

The use of autonomous sensors for analyzing wide bands of radio frequency spectrum requires using the high-speed analog-to-digital converters (ADC). The operation of such devices with high bit resolution requires several watts of power. One-bit ADC will reduce power consumption and simplify the analog part of the receiver. The goal of the research is to determine the features and conditions under which it is advisable to analyze the radio frequency spectrum in a sophisticated radio electronic environment using a one-bit ADC. The problem of using such ADC is the deterioration of the signal-to-noise ratio (SNR) and the occurrence of spurious spectral components at its' medium and high values. The task of spectrum sensing is complicated by the fact that a large number of signals with different values of bandwidth and SNR can be simultaneously present in the analyzed frequency band. After a one-bit ADC, the energy of the complex signal remains unchanged regardless of its shape. Therefore, at high SNR values, the signal energy flows into spurious spectral components. When the bandwidth of the signal increases to 30% of analyzed frequency range and higher, the spurious spectral components are transformed into a broadband pedestal. Analytical dependencies have been obtained that allow us to calculate the values of the SNR at which signals can be detected and spurious spectral components appear. These dependencies take into account the parameters of the Welch periodogram and the level of spectrum occupancy. The results of the analysis of real signals showed that the shape of the signal spectrum after one-bit ADC repeats the shape of the spectrum after an 8-bit ADC, except for the absence of some weak signals. The cost for simplified hardware implementation and lower power consumption when using one-bit ADC compared to ADC with higher resolution is a narrowing of the dynamic range of signals. The use of one-bit ADC for spectrum sensing will be justified only when there is information on the analyzed bandwidth occupancy and the SNR of the signals that can be observed.

Keywords: spectrum sensing; spurious spectral components; one-bit quantization; radio monitoring; dynamic range

DOI: 10.20535/RADAP.2024.97.20-29

Introduction

Nowadays, radio spectrum sensing is increasingly performed using networks of autonomous sensors [1, 2], including those placed on unmanned vehicles. In such conditions, the task is in increasing the autonomy of radio monitoring devices by reducing their power consumption. Analysis of wide bandwidth requires the use of high-speed analog-to-digital converters (ADC). The operation of such devices with high bit resolution requires several watts of power. In particular, at a sampling rate of 3.2 GHz/s, the power consumption for an 8-bit ADC is 105 mW, and for a single-bit ADC, it is only 20 μW [3, 4]. One-bit ADC can be implemented using high-speed comparators. For spectrum sensing, this solution is quite attractive due to its low cost, low power consumption, and high sampling rate. This is achieved at the expense of some deterioration in system performance due to the loss of some information (the signal is quantized by only two levels, usually +1 and -1, and can be represented by only one bit of data). The use of one-bit ADC will simplify the analog part of the receiver due to a significant narrowing of the dynamic range of the input signal. In particular, there is no need for automatic gain control [5] because the risk of signal saturation and clipping disappears. Therefore, the study of spectrum sensing peculiarities using one-bit ADC for small-sized broadband autonomous radio monitoring devices is an urgent scientific and applied task.

1 Related works

The issues of signal processing in low-bit quantization are considered in numerous works devoted to the study of communication systems, radar systems, and radio monitoring systems.

In [6–16], it was proposed to use one-bit ADC to reduce the power consumption and complexity of the hardware of MIMO base stations. It is shown that this approach practically does not degrade the quality of the system. It is shown in [17] that 2-3 bits are sufficient to solve most signal processing tasks. Processing losses when using a low-bit ADC increase with an increase in the signal-to-noise ratio (SNR). Therefore, ADCs

with bit resolution of more than 3 bits are advisable to use for medium and high SNR values. The use of one-bit ADC in radar systems reduces their cost and power consumption [18]. In [19], a signal pre-processing algorithm is proposed to reduce higher-order spurious harmonics, which is especially relevant for the case of simultaneous observation of several targets. It is shown that for low values of SNR, processing gain is about 1.3 dB, and at high SNR, the losses are about 1 dB. In [20], as a result of analytical calculations, the value of processing losses for the case of an unquantized signal and a quantized one-bit signal was obtained at the level of 2 dB.

In [21, 22], it is shown that the losses of a one-bit ADC are about 2 dB and can be compensated by increasing the sample size by 2.47 times. In [23], it is shown that a few bits of ADC resolution are sufficient to obtain adequate estimates of the frequency spectrum even for a complex signal environment. A broadband radio monitoring system is proposed in [24, 25]. It is shown that the use of one-bit data greatly simplifies the hardware implementation of fast Fourier transform (FFT) modules and a signal detector. In [26], it is shown that the use of 2-3 bits in spectrum sensing provides almost the same results as processing an unquantized signal. In [27], an approach is proposed to detect unoccupied frequencies when processing one-bit signal samples. In [28], it is shown that it is possible to obtain adequate estimates of the power spectral density (PSD) using several bits even at high band occupancy.

2 Problem statement

The results of publications analysis show that the issues of assessing the effect of one-bit quantization on spectrum sensing under conditions of high occupancy and wide dynamic range of signals, in particular, the creation of spurious spectral components arising at high SNR, remain unexplored. In particular, there is no information on the influence of the number of signals in the analyzed frequency band, their SNR, and spectrum occupancy on the detection characteristics of these signals. The limits of the values of signal parameters at which it is advisable to analyze spectrum using a one-bit ADC have not been investigated.

The aim of the research is to determine the peculiarities and conditions under which it is advisable to accomplish spectrum sensing in sophisticated radio-electronic environment using one-bit ADC.

3 One-bit ADC search for spectrum sensing

The problem with using low-bit, in particular one-bit, ADCs is the SNR deterioration and the occurrence of spurious spectral components at medium and high SNR values. These spectral components can be either harmonics or non-harmonics of the input signal. Moreover, the fewer bits of the ADC and lower the SNR, the more spurious components are observed [29]. The appearance of such harmonics in the detection of signals in the frequency domain leads to false detections, especially if there are several signals with different powers in the analyzed frequency band at the same time.

To deal this negative phenomenon, a randomization process is used, which consists in adding noise to the analog signal before the ADC. This method produces a noisy analog signal that more clearly crosses the quantization level boundaries of the least significant bit of the ADC. After that, the quantization noise becomes more random and with a reduced level of unwanted harmonic components. Randomization increases the average noise level in the frequency domain, but improves the SNR, since it destroys the correlation of the quantization noise with the input signal and an averaging operation can be performed. It is advisable to use randomization when converting low-level analog signals, periodic analog signals, and slowly changing signals [29].

The maximum SNR of an ideal b-bit ADC in dB can be calculated according to the following expression [29]:

$$SNR = 6.02b + 4.77 + 20\lg(LF), \quad (1)$$

where the first term corresponds to the dynamic range of the ADC, and LF is the utilization factor calculated as:

$$LF = \sigma_s / 2V_p, \quad (2)$$

where σ_s – the root mean square value of the input signal; $2V_p$ – full range of the ADC input signal.

In accordance with expression (1), the maximum SNR value will be at $\sigma_s = V_p$ and will be $(6.02b + 1.76)$ dB. Real ADCs, taking into account additional noise sources, have a SNR value 3-6 dB lower than that calculated by expression (1). Increasing the sampling rate by a factor of 4 provides the same gain in SNR as increasing the ADC bit depth by 1 bit.

A one-bit ADC distorts the signal because it takes the $sign()$ function from the real and imaginary components of the complex signal and thus removes all information about the signal amplitude. The complex signal at the output of a one-bit ADC can be written in the following form:

$$x(n) = sign(s(n)) = sign(I_n + jQ_n) = \pm 1 \pm j1, \quad (3)$$

where $sign()$ – a function that returns 1 if the argument is positive, -1 for a negative argument, and 0 if the argument is 0.

To combat such distortions in massive MIMO systems, noise with a certain power is added to the received signal [8–10]. The implementation of this approach becomes possible due to the known limits of signals dynamic range in the system. However, for radio

monitoring systems, the dynamic range of signals and, accordingly, the SNR value for each signal can vary within a wide range, and adding noise to the received signal can both improve and degrade the system performance. Therefore, in spectrum sensing tasks, it is necessary to control the SNR so that its value is within the operating range. This task is complicated by the fact that a large number of signals with different bandwidth and SNR can be simultaneously present in the analyzed frequency band.

In Fig. 1 is shown the dependence of the noise level in the frequency domain for a one-bit ADC on the SNR for a harmonic and a frequency-modulated signal at different values of the ratio of the signal bandwidth Δf to the analyzed frequency band $\Delta\Pi = F_s$ (F_s = 10 MHz) η. The variance of the complex Gaussian noise with zero mean was 2. The SNR value in the time domain can be estimated by the following expression:

$$SNR_t = \frac{\sigma_s^2}{\sigma_\xi^2}, \tag{4}$$

where σ_s^2, σ_ξ^2 – signal and noise variances, respectively.

Accordingly, the SNR in the frequency domain can be approximated as the ratio of signal power to noise level or using the values of SNR_t, the bandwidth of the complex signal, and the sampling rate:

$$SNR_f \approx 10\lg(SNR_t) + 10\lg\left(\frac{F_s}{\Delta f}\right) \approx \approx 10\lg(SNR_t) - 10\lg(\eta). \tag{5}$$

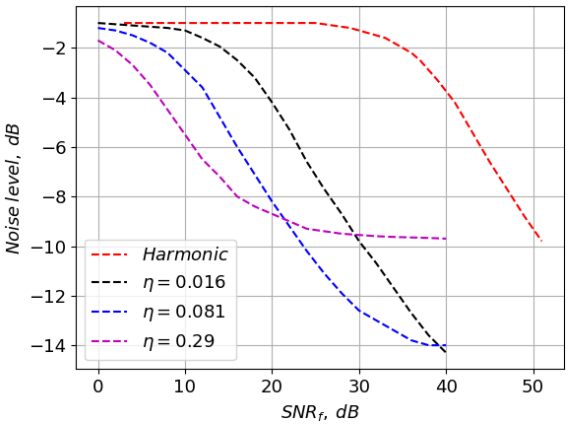

Fig. 1. Dependence of noise level in frequency domain for one-bit ADC on SNR

The PSD of complex signal samples was calculated for the following parameters of the Welch periodogram: the length of the FFT window is N_{FFT} = 16384, the overlap between adjacent windows is $R = N_{FFT}/2$, the number of accumulated periodograms is M = 30, and the type of window function is Hamming. In this case, the number of samples to be analyzed is $N = N_{FFT} + (M-1)R$. In the absence of a signal, the noise level for both the one-bit ADC and the 12-bit ADC are the same and in this case are about minus 1 dB. As the SNR increases, the noise level of a one-bit ADC decreases. This is due to the fact that noise components with low amplitude will be superimposed mainly on large signal values, not those close to 0, and will be rejected during one-bit quantization. With an increase in the relative width of the signal spectrum η, the SNR value at which a sharp decrease in noise level begins decreases.

Fig. 2a shows PSD of harmonic at SNR of -10 dB, and Fig. 2b at a SNR of 20 dB over the entire frequency band. As we can see, with SNR increasing, a large number of spurious harmonics appear, and the level of the useful spectral component and the noise level decrease. This is due to the transformation of the harmonic signal into a meander with values of 1 and -1, which leads to the rejection of more and more energy of both signal and noise with SNR increasing.

In this case, the spurious spectral components begin to appear at an SNR of about -5 dB. The spectral component that corresponds to the signal has the maximum power and is easy to distinguish. However, this situation will change when there are several signals with different powers in the analyzed frequency band and it will be almost impossible to detect useful signals.

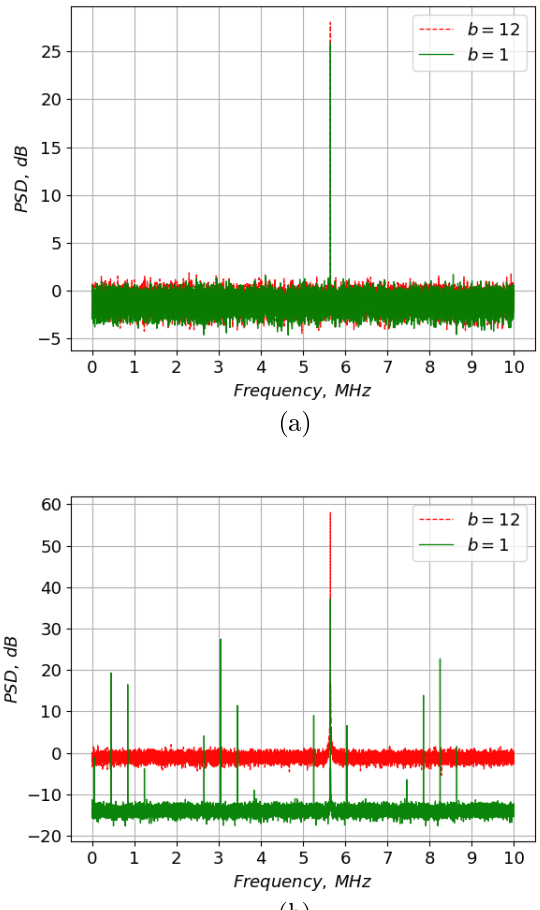

Fig. 2. Harmonic PSD for SNR -10 dB (a) and 20 dB (b)

In Fig. 3a is shown the dependence of the SNR in time domain, at which it is possible to detect a harmonic signal (lower group of lines) and the appearance of a spurious spectral component (upper group of lines), on the length of the FFT window at different values of the number of averaged periodograms M. When the length of the FFT window is doubled, the gain in SNR in the frequency domain when detecting a signal is about 3 dB, regardless of the number of accumulated realizations of the FFT M. Also, when the N_{FFT} is doubled, the SNR value at which spurious spectral components appear decreases by about 1 dB. Increasing the integration time (FFT length) by a factor of 4 reduces the noise amplitude by a factor of 2 or by 6 dB (3 dB in power), which is equivalent to 1 additional ADC bit.

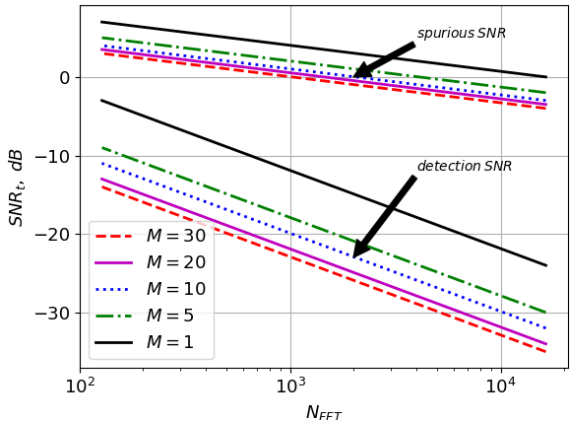

(a)

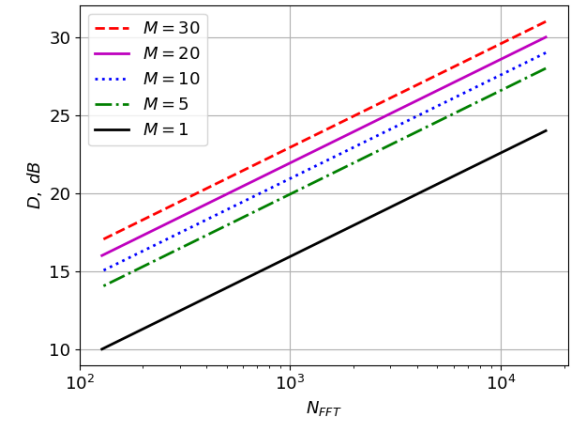

(b)

Fig. 3. SNR dependency, at which it is possible to detect harmonics and the appearance of spurious components (a), and dynamic range (b) on FFT length

The approximate dependence of the SNR in dB, at which it is possible to detect a harmonic signal for a one-bit ADC, on the length of the FFT window N_{FFT} and the number of implementations of the FFT M, can be written in accordance with the following expression:

$$SNR_{\text{det}}\,(N_{FFT}, M) \approx -4.3\ln(N_{FFT}) - 7.56\lg(M) + 18. \quad (6)$$

Similarly to (6), we can write an expression for the SNR in dB, at which spurious spectral components appear:

$$SNR_{spur}(N_{FFT}, M) \approx -1.44\ln(N_{FFT}) - 2.7\lg(M) + 14. \quad (7)$$

These expressions were obtained by author for the Hamming window function. For other types of windows, the appropriate loss factor should be used [30].

Fig. 3b shows the dependence of the dynamic range D on the N_{FFT} for different M, at which it is possible to detect a harmonic signal without the risk of spurious spectral components.

Subtracting expression (6) from expression (7), we can obtain an equation for calculating the dynamic range D in dB for harmonic detection:

$$D \approx 4.86\lg(M) + 2.86\ln(N_{FFT}) - 4. \quad (8)$$

Expressions (6)-(8) were obtained for values of the FFT window lengths in the range from 128 to 16384.

Thus, the cost for simplifying the hardware implementation and lower power consumption when using a one-bit ADC compared to an ADC of higher bit resolution is a narrowing of the dynamic range of signals. These limitations are due to the rejection of part of the signal energy due to one-bit quantization and the spreading of signal energy over spurious spectral components.

Compared to an unquantized signal, the loss in the SNR of a one-bit ADC when detecting signals is about 2 dB, regardless of the periodogram parameters. This is because one-bit quantization reduces both the signal and noise levels, and the difference between these levels remains almost unchanged. This statement is true for those SNR in which spurious spectral components do not yet appear and the signal energy does not spread over them.

With an increase in the relative signal bandwidth η, the SNR_{det} value at which signal detection is possible and the spurious spectral components SNR_{spur} appear increases. When the N_{FFT} is changed from 16384 to 128, a signal with $\eta = 0.1$ can be detected at SNR values ranging from -13 dB to -9 dB, and spurious spectral components appear at SNRs from 5 dB to 8 dB.

Also, with an increase in η, the dynamic range within which operation is possible without the appearance of spurious spectral components became narrower. The value of the dynamic range practically does not depend on the parameters of the Welch periodogram and for $\eta = 0.1$ is about 17 dB.

In Fig. 4a is shown the PSD of the signal at a SNR of 20 dB with a value of $\eta = 0.1$ for $N_{FFT} = 16384$ and $M = 30$, and Fig. 4b – at $\eta = 0.3$. The PSD is

shown for a one-bit and 12-bit ADC. From Fig. 4a it is evident that with an increase in the number of the spurious component, its amplitude decreases and the bandwidth increases. In Fig. 4b, the spurious spectral components have generally turned into a continuous noise-like pedestal. This effect is manifested at $\eta > 0.3$. In this case, the risk of spurious spectral components disappears. The SNR at which the spurious spectral components appear for $\eta \approx 0.3$ can be estimated approximately by expression (7) by adding 9 dB to it.

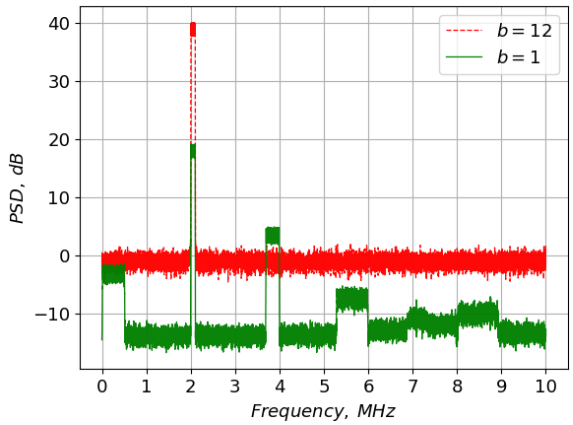

(a)

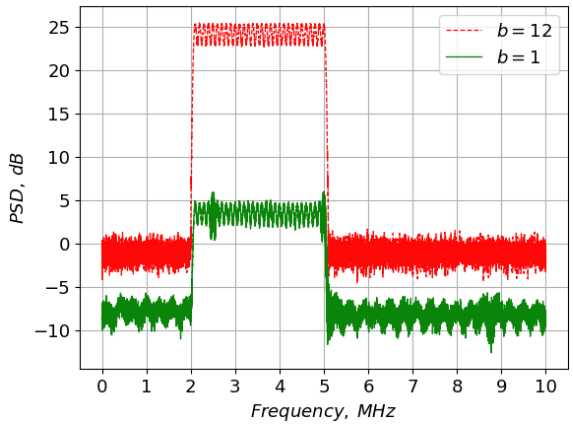

(b)

Fig. 4. PSD for $\eta = 0,01$ (a) and $\eta = 0,3$ (b) for SNR 20 dB

Fig. 5a shows the dependence of the signal strength in the frequency domain on the SNR for different values of the relative signal bandwidth for a one-bit and a 12-bit ADC. In the latter case, the signal strength in the frequency domain increases linearly for all values of the SNR.

For a one-bit ADC, at a certain value of SNR, the signal level practically stops growing. Moreover, the larger η, the lower the SNR when its' growth stops. A similar behavior is observed for the dependencies of the SNR (Fig. 5b). For a 12-bit ADC, the relationship between these quantities is almost linear. For a one-bit ADC, the SNR in the frequency domain also grows almost linearly up to a certain value of SNR, after which the growth rate slows down and then stops altogether.

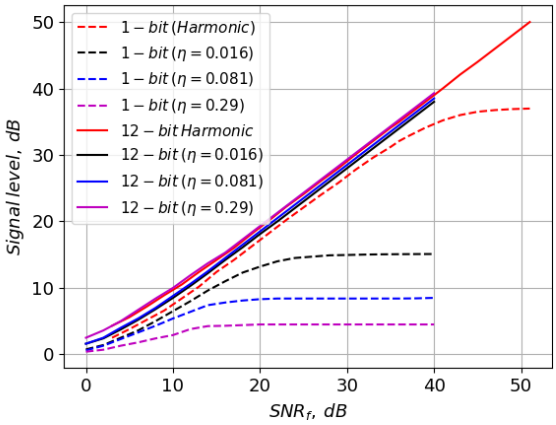

(a)

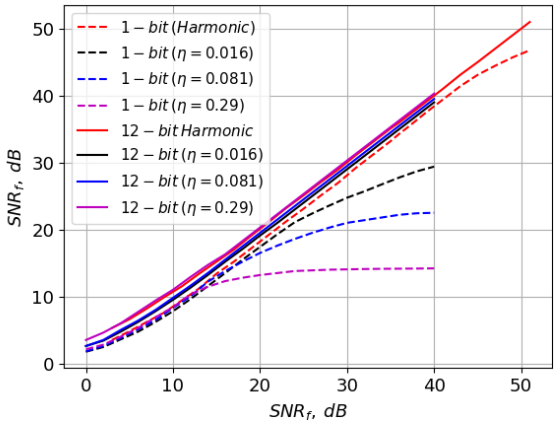

(b)

Fig. 5. Signal level (a) and SNR dependencies in frequency domain (b) on SNR in time domain

In sophisticated electronic environment, when the analyzed frequency band contains signals with different types of modulation, different bandwidths, and approximately equal powers, the total received signal will be noise-like. In this case, the spurious spectral components appear at higher SNR than for individual signals with a given bandwidth (expression (7)). In this case, the value of occupancy η can be written in the following form:

$$\eta \approx \frac{\sum_{i=1}^{K} \Delta f_i}{\Delta \Pi}. \qquad (9)$$

However, when there is one component in the signal mixture with a much higher SNR than for other signals, there is a risk of spurious spectral components.

As a generalization of the previous calculations, Fig. 6 shows approximate graphs of the SNR dependence in the time domain, at which it is possible to detect the signal $SNR_{det}(\eta)$ and the spurious spectral components $SNR_{spur}(\eta)$ appear for $N_{FFT} =$

1024 and $M = 10$ (a) and $N_{FFT} = 16384$ and $M = 30$ (b). The area shaded between these curves for each value of η corresponds to the dynamic range in which unambiguous signal detection is possible. It can be seen from these graphs that the value of the dynamic range expands with increasing the length of the FFT window. Also, when η increases to values around 0.2, the dynamic range became narrower. For $\eta > 0.2$, the value of D remains almost unchanged.

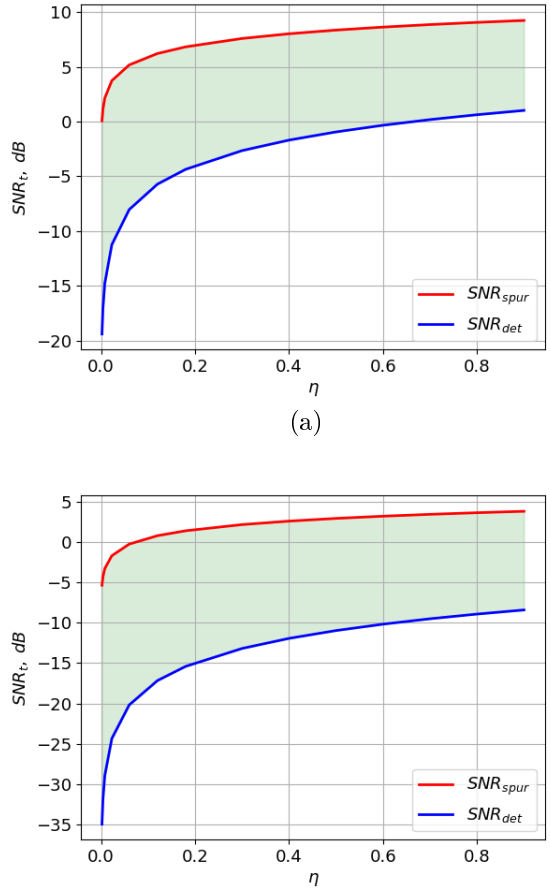

(a)

(b)

Fig. 6. Dependency of SNR_{det}, SNR_{spur} from η for $N_{FFT} = 1024$, $M = 10$ (a) and $N_{FFT} = 16384$, $M = 30$ (b)

Taking into account equations (5)-(6), the value of the SNR at which signal detection is possible can be written in accordance with the following expression

$$SNR_{\text{det}}\left(N_{FFT}, M, \eta\right) \approx \approx \ln(N_{FFT})\left(1.15\lg(\eta) - 1.2\right) - 7.56\lg(M) + 18. \quad (10)$$

Similarly, taking into account expression (7), we can write down the dependence of the SNR at which spurious spectral components appear:

$$SNR_{spur}\left(N_{FFT}, M, \eta\right) \approx \approx -1.44\ln(N_{FFT}) - 2.7\lg(M) + 1.5ln(\eta) + 24.5. \quad (11)$$

From these dependences, it can be concluded that under conditions of a priori uncertainty about the radio electronic environment, in order to reduce the risk of spurious spectral components due to the high value of the SNR, it is advisable to choose small values of N_{FFT} and as large values of M as possible.

In Fig. 7a is shown the spectra for a harmonic signal and two frequency-modulated signals with relative bandwidths of 0.1 and 0.3, respectively, and a SNR of 5 dB for each signal. The parameters of the Welch periodogram are for $N_{FFT} = 1024$ and $M = 30$. In Fig. 7b is shown a similar graph for the case when the SNR of the harmonic signal is 25 dB. As we can see, the appearance of a powerful harmonic signal completely masks other signals and creates harmonic spurious spectral components.

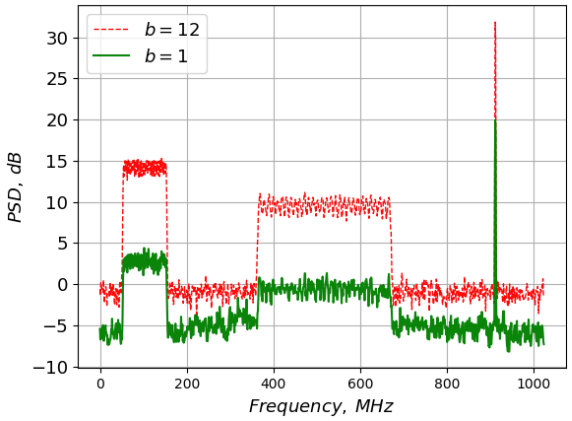

(a)

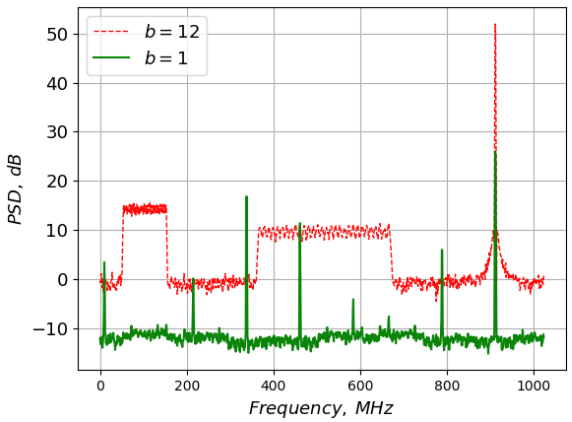

(b)

Fig. 7. PSD for harmonic with SNR of 5 dB (a) and 25 dB (b)

In Fig. 8a is shown the PSD for the previous signal environment at SNR 35 dB for a signal with $\eta = 0.1$. This signal almost completely masked the harmonic and created a set of spurious spectral components in the form of two broadband signals. At a SNR of 35 dB for a signal with $\eta = 0.3$ (Fig. 8b), the remaining signals are completely masked by a wide pedestal.

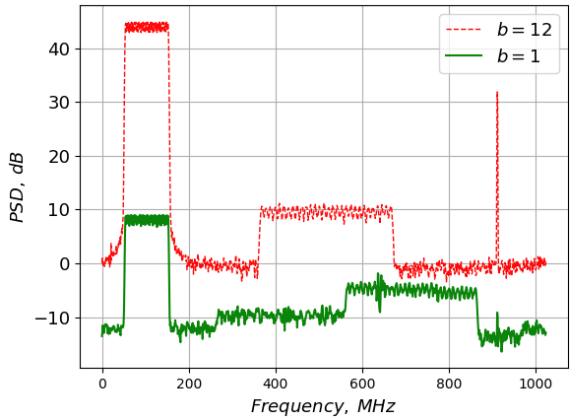

(a)

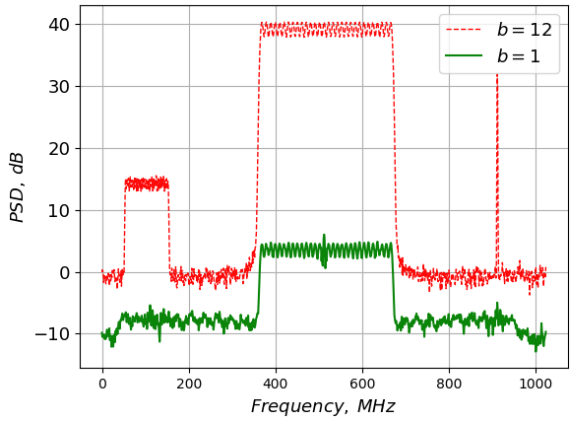

(b)

Fig. 8. PSD for 35 dB SNR for signal with $\eta = 0.1$ (a) and $\eta = 0.3$ (b)

Since after a one-bit ADC the energy of the complex signal remains unchanged and amounts to $2N$ regardless of its shape, at high values of the SNR, the signal flows into spurious spectral samples where the signal is absent. However, at a certain value of the SNR, this process stops and the PSD will remain practically unchanged with further increase of the SNR. This phenomenon is observed for $\eta > 0.3$. For this case, the noise level does not decrease with increasing SNR, since the energy of the spurious spectral components forms an almost continuous pedestal in the entire frequency band. Thus, for $\eta = 0.3$, with an increase of SNR, the difference between the signal and noise levels is about 12 dB. At $\eta = 0.5$, this difference is 10 dB, and for $\eta = 0.8 - 8$ dB. Moreover, with an increase in N_{FFT}, these ratios remain almost unchanged. For the case of a harmonic signal, with an increase in the SNR, the noise level decreases and additional spectral components appear. The powers of the remaining components remain unchanged.

For a one-bit ADC, the moments of time when the signal value is zero are significant (expression (3)). Since the signal amplification operation does not affect these moments of time, the use of a logarithmic amplifier to narrow the dynamic range of signals will be appropriate only if you use an ADC with more than 1 bit.

Under conditions of a priori uncertainty about the received signals' SNR and bandwidth, which are typical conditions for spectrum sensing, adding noise to the received signal in the entire analyzed frequency band can either improve or degrade the performance of signal detection algorithms. The same applies to the case of adding noise only in some part of the analyzed frequency band. In this case, the risk of spurious combination spectral components arising from the superposition of bandpass noise and received signals increases. Moreover, the parameters of the spurious components depend on the amplitude, frequency, and phase relations between the parameters of the received signals and noise.

The SNR can also be reduced by adjusting the signal gain before the ADC. However, in this case, it is necessary to measure the noise and signal levels, which will complicate the technical implementation of the spectrum analyzer.

4 Real life radio electronic environment analysis

The signal was recorded using a software-defined radio receiver HackRF One in the 20 MHz band with a resolution of 8 bits. Before calculating the PSD, the recorded quadrature signal was transformed according to expression (3), which simulates the operation of a one-bit ADC. In Fig. 9a is shown the PSD of DVB-T2 digital television signals, and Fig. 9b – GSM and 4G LTE signals in the 900 MHz band. For comparison, these graphs show the PSD of signals after 8-bit ADC. As can be seen from these spectra, the distortion introduced by a one-bit ADC is to reduce the SNR of the signals in the frequency domain. It is also worth noting that the shape of the signal spectrum after one-bit ADC repeats the shape of the spectrum after an 8-bit ADC, except for the absence of some weak signals.

Figure 10a shows the PSD of 4G LTE signals in the 1800 MHz frequency range and 3G UMTS signals in the 2100 MHz frequency range (Fig. 10b). Despite the high SNR for both signals, spurious spectral components are not clearly observed, and the distortion of the PSD is manifested in a decrease in signal levels. The PSD in Figs. 9-10 are calculated for $N_{FFT} = 1024$ and $M = 30$.

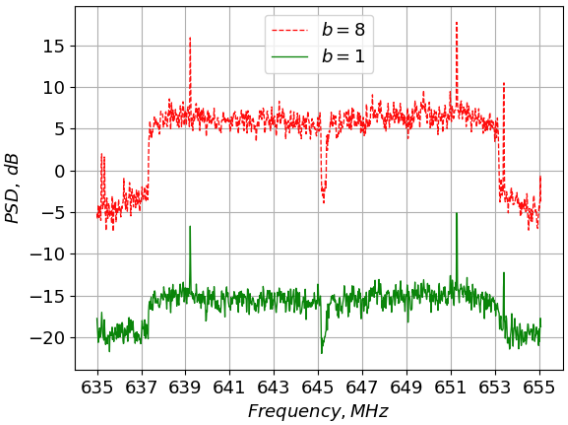

(a)

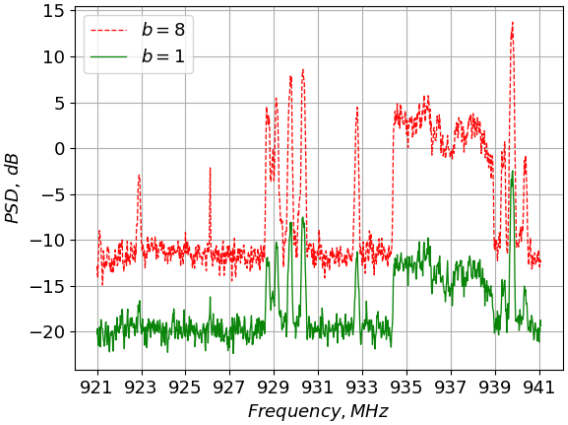

(b)

Fig. 9. PSD DVB-T2 (a) and GSM with 4G LTE (b)

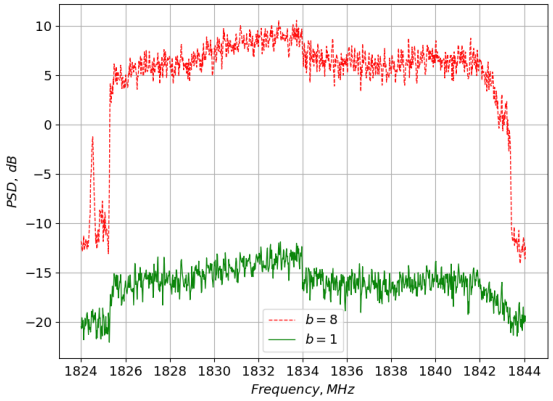

(a)

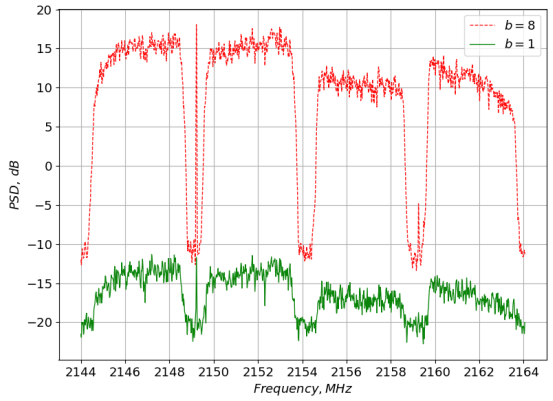

(b)

Fig. 10. PSD 4G LTE (a) and 3G UMTS (b)

Figures 11 shows the PSD for the frequency range of 935-965 MHz for the FFT window lengths $N_{FFT} = 1024$ (a) and $N_{FFT} = 16384$ (b) and $M = 30$. Due to the high SNR of some signals, there is a significant distortion of the PSD, which is manifested in the complete masking of some, even relatively powerful signals, and a change in the spectrum shape in the analyzed frequency band.

Thus, the use of a one-bit ADC for spectrum sensing will be justified only when there is information on the analyzed frequency bandwidth and the SNR of the signals that can be observed. Then, using expressions (10)-(11), it is possible to obtain the values of the parameters of the Welch periodogram, at which it is possible to calculate the PSD in the analyzed frequency band without the appearance of spurious spectral components.

Conclusions

The scientific novelty of the results obtained is the determination of analytical dependencies that allow to calculate the values of the SNR at which signals can be detected and spurious spectral components appear. These dependencies take into account only the parameters of the Welch periodogram and the level of spectrum occupancy. In general, SNR value must not be greater than 5-10 dB for all occupancy levels. It is shown that the use of one-bit ADC for spectrum sensing will be justified only when there is information on the occupancy of the analyzed frequency band and the SNR of the signals that can be observed. The results obtained in the study do not contradict the results presented in [17,20,27] and provide justification for the feasibility of using one-bit ADC for spectrum sensing.

Prospects for further research in this area are to study the possibility of reconstructing signals in the time domain after bandpass filtering of signals detected in the frequency domain.

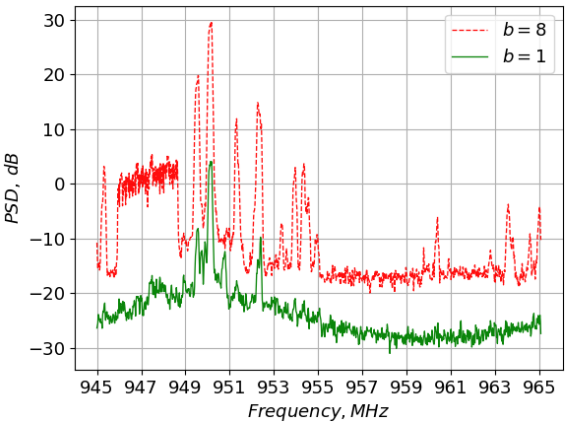

(a)

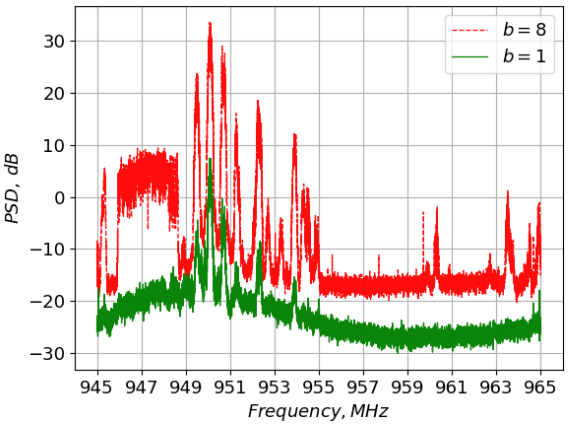

(b)

Fig. 11. PSD for $N_{FFT} = 1024$ (a) and $N_{FFT} = 16384$ (b)

References

[1] Zayyani H., Haddadi F., Korki M. (2020). One-Bit Spectrum Sensing in Cognitive Radio Sensor Networks. *Circuits Syst Signal Process*, Vol. 39, pp. 2730–2743, doi: 10.1007/s00034-019-01274-z.

[2] Deng J., Chen Y. (2019). Subspace-based 1-bit Wideband Spectrum Sensing. *11th International Conference on Wireless Communications and Signal Processing (WCSP)*, pp. 1-6, doi: 10.1109/WCSP.2019.8928133.

[3] Mishali M., Eldar Y. C., Dounaevsky O., and Shoshan E. (2011). Sampling: Analog to digital at sub-Nyquist rates. *IET Circuits, Devices & Systems*, Vol. 5, Iss. 1, pp. 8–20, doi: 10.1049/iet-cds.2010.0147.

[4] Rivet F., Deval Y., Begueret J.-B., Dallet D., Cathelin P. and Belot D. (2010). The Experimental Demonstration of a SASP-Based Full Software Radio Receiver. *IEEE Journal of Solid-State Circuits*, Vol. 45, Iss. 5, pp. 979-988, doi: 10.1109/JSSC.2010.2041402.

[5] Graf O., Bhandari A. and Krahmer F. (2019). One-bit Unlimited Sampling. *ICASSP 2019-2019 IEEE International Conference on Acoustics, Speech and Signal Processing (ICASSP)*, pp. 5102-5106, doi: 10.1109/ICASSP.2019.8683266.

[6] Mollén C., Choi J., Larsson E. G. and Heath R. W. (2017). Uplink Performance of Wideband Massive MIMO With One-Bit ADCs. *IEEE Transactions on Wireless Communications*, Vol. 16, Iss. 1, pp. 87-100, doi: 10.1109/TWC.2016.2619343.

[7] Jacobsson S., Durisi G., Coldrey M., Gustavsson U. and Studer C. (2015). One-bit massive MIMO: Channel estimation and high-order modulations. *IEEE International Conference on Communication Workshop (ICCW)*, pp. 1304-1309, doi: 10.1109/ICCW.2015.7247358.

[8] Jacobsson S., Durisi G., Coldrey M., Gustavsson U. and Studer C. (2017). Throughput Analysis of Massive MIMO Uplink With Low-Resolution ADCs. *IEEE Transactions on Wireless Communications*, Vol. 16, Iss. 6, pp. 4038-4051, doi: 10.1109/TWC.2017.2691318.

[9] Li Y., Tao C., Seco-Granados G., Mezghani A., Swindlehurst A. L. and Liu L. (2017). Channel Estimation and Performance Analysis of One-Bit Massive MIMO Systems. *IEEE Transactions on Signal Processing*, Vol. 65, Iss. 15, pp. 4075-4089, doi: 10.1109/TSP.2017.2706179.

[10] Desset C., Van der Perre L. (2015). Validation of low-accuracy quantization in massive MIMO and constellation EVM analysis. *European Conference on Networks and Communications (EuCNC)*, pp. 21-25, doi: 10.1109/EuCNC.2015.7194033.

[11] Sarajlić M., Liu L. and Edfors O. (2017). When Are Low Resolution ADCs Energy Efficient in Massive MIMO? *IEEE Access*, Vol. 5, pp. 14837-14853, doi: 10.1109/ACCESS.2017.2731420.

[12] Verenzuela D., Björnson E. and Matthaiou M. (2017). Per-antenna hardware optimization and mixed resolution ADCs in uplink massive MIMO. *51st Asilomar Conference on Signals, Systems, and Computers, Pacific Grove*, pp. 27-31, doi: 10.1109/ACSSC.2017.8335129.

[13] Nguyen L. V., Swindlehurst A. L. and Nguyen D. H. N. (2021). SVM-Based Channel Estimation and Data Detection for One-Bit Massive MIMO Systems. *IEEE Transactions on Signal Processing*, Vol. 69, pp. 2086-2099, doi: 10.1109/TSP.2021.3068629.

[14] Dong Y., Wang H. and Yao Y.-D. (2021). Channel Estimation for One-Bit Multiuser Massive MIMO Using Conditional GAN. (2021). *IEEE Communications Letters*, Vol. 25, Iss. 3, pp. 854-858, doi: 10.1109/LCOMM.2020.3035326.

[15] Shao M., Li Q., Ma W.-K. and So A. M.-C. (2019). A Framework for One-Bit and Constant-Envelope Precoding Over Multiuser Massive MISO Channels. *IEEE Transactions on Signal Processing*, Vol. 67, Iss. 20, pp. 5309-5324, doi: 10.1109/TSP.2019.2937280.

[16] Liu J., Luo Z. and Xiong X. (2019). Low-Resolution ADCs for Wireless Communication: A Comprehensive Survey. *IEEE Access*, Vol. 7, pp. 91291-91324, doi: 10.1109/ACCESS.2019.2927891.

[17] Shi B. et al. (2022). Impact of Low-Resolution ADC on DOA Estimation Performance for Massive MIMO Receive Array. *IEEE Systems Journal*, Vol. 16, Iss. 2, pp. 2635-2638, doi: 10.1109/JSYST.2021.3139449.

[18] Ameri A., Bose A., Li J. and Soltanalian M. (2019). One-Bit Radar Processing With Time-Varying Sampling Thresholds. *IEEE Transactions on Signal Processing*, Vol. 67, Iss. 20, pp. 5297-5308, doi: 10.1109/TSP.2019.2939086.

[19] Jin B., Zhu J., Wu Q., Zhang Y. and Xu Z. (2020). One-Bit LFMCW Radar: Spectrum Analysis and Target Detection. *IEEE Transactions on Aerospace and Electronic Systems*, Vol. 56, Iss. 4, pp. 2732-2750, doi: 10.1109/TAES.2020.2978374.

[20] Xiao Y.-H., Ramírez D., Schreier P. J., Qian C. and Huang L. (2022). One-Bit Target Detection in Collocated MIMO Radar and Performance Degradation Analysis. *IEEE Transactions on Vehicular Technology*, Vol. 71, Iss. 9, pp. 9363-9374, doi: 10.1109/TVT.2022.3178285.

[21] Wu P.-W. et al. (2023). One-Bit Spectrum Sensing for Cognitive Radio. *Electrical Engineering and Systems Science-Signal Processing*, 13 p. doi: 10.48550/arXiv.2306.13558.

[22] Zhao Y., Ke X., Zhao B., Xiao Y. and Huang L. (2021). One-Bit Spectrum Sensing Based on Statistical Covariances: Eigenvalue Moment Ratio Approach. *IEEE Wireless Communications Letters*, Vol. 10, Iss. 11, pp. 2474-2478, doi: 10.1109/LWC.2021.3104346.

[23] Mehanna O., Sidiropoulos N. D. (2013). Frugal Sensing: Wideband Power Spectrum Sensing From Few Bits. *IEEE Transactions on Signal Processing*, Vol. 61, Iss. 10, pp. 2693-2703, doi: 10.1109/TSP.2013.2252171.

[24] Ali A., Hamouda W. (2016). Low Power Wideband Sensing for One-Bit Quantized Cognitive Radio Systems. *IEEE Wireless Communications Letters*, Vol. 5, Iss. 1, pp. 16-19, doi: 10.1109/LWC.2015.2487347.

[25] Merlano-Duncan J. C., Sharma S. K., Chatzinotas S., Ottersten B. and Wang X. (2017). Multi-antenna based one-bit spatio-temporal wideband sensing for cognitive radio networks. *IEEE International Conference on Communications (ICC)*, pp. 1-7, doi: 10.1109/ICC.2017.7996737.

[26] Nguyen L. L., Nguyen D. H. N., Fiche A., Huynh T. and Gautier R. (2019). Low-Bit Quantization Methods for Modulated Wideband Converter Compressed Sensing. *IEEE Global Communications Conference (GLOBECOM)*, pp. 1-6, doi: 10.1109/GLOBECOM38437.2019.9013470.

[27] Libin M. K., Shreejith S., Vinod A. P. and Madhukumar A. S. (2020). A Power-Efficient Spectrum-Sensing Scheme Using 1-Bit Quantizer and Modified Filter Banks. *IEEE Transactions on Very Large Scale Integration (VLSI) Systems*, Vol. 28, Iss. 9, pp. 2074-2078, doi: 10.1109/TVLSI.2020.3009430.

[28] Chen Y., Zhao Y., Huang J., and Zheng Y. (2019). Multiband sparse signal reconstruction through direct one-bit sampling. *Rev. Sci. Instrum.*, Vol. 90, Iss. 8, pp. 2693-2703, doi: 10.1063/1.5113925.

[29] Lyons R. G. (2011). *Understanding Digital Signal Processing*, 3rd ed. Prentice Hall, 858 p.

[30] Prabhu K. M. M. (2014). Window functions and their applications in signal processing. *Taylor&FrancisGroup*, LLC, 406 p. doi: 10.1201/9781315216386.

Особливості аналізу радіочастотного спектра при використанні однобітного аналого-цифрового перетворення

Бугайов М. В.

Використання автономних сенсорів для аналізу широких смуг радіочастотного спектра вимагає використання високошвидкісних аналого-цифрових перетворювачів (АЦП). Робота таких пристроїв із високою розрядністю потребує потужності кілька Вт. Використання однобітних АЦП дозволить зменшити споживану потужність та спростити аналогову частину приймача.

Метою досліджень є визначення особливостей та умов, при яких доцільно аналізувати радіочастотний спектр в умовах складної радіоелектронної обстановки із використанням однобітного АЦП. Проблема використання таких АЦП полягає у погіршенні відношення сигнал-шум (ВСШ) та виникненні паразитних спектральних складових при середніх та високих його значеннях. Завдання радіомоніторингу ускладнюється тим, що в смузі частот аналізу може перебувати одночасно велика кількість сигналів з різними значеннями ширини спектра та ВСШ.

Після однобітного АЦП енергія комплексного сигналу залишається незмінною незалежно від його форми. Тому при високих значеннях ВСШ спостерігається перетікання сигналу у паразитні спектральні складові. При збільшенні ширини спектра сигналу до 30% від ширини смуги аналізу і вище паразитні спектральні складові перетворюються у суцільний широкосмуговий п'єдестал. Отримано аналітичні залежності, що дозволяють розраховувати значення ВСШ, при яких можливе виявлення сигналів та з'являються паразитні спектральні складові. Дані залежності враховують параметри періодограми Уелча та рівень завантаженості. Результати аналізу реальних сигналів показали, що форма спектра сигналу після однобітного АЦП повторює форму спектра після 8-бітного АЦП за винятком відсутності деяких слабких сигналів. Платою за спрощення апаратної реалізації та менші енергозатрати при використанні однобітного АЦП в порівнянні з АЦП більшої розрядності є звуження динамічного діапазону сигналів. Використання однобітного АЦП для ведення радіомоніторингу буде оправданим лише в умовах, коли є інформація щодо завантаженості смуги частот аналізу та ВСШ сигналів, які можуть спостерігатися.

Ключові слова: радіочастотний спектр; паразитні спектральні складові; однобітне квантування; радіомоніторинг; динамічний діапазон